Video Article

A Silver Nanoparticle Method for Ameliorating Biliary Atresia Syndrome in Mice

Ming Fu[1], Zefeng Lin[2], Huiting Lin[2], Yanlu Tong[2], Hezhen Wang[2], Hongjiao Chen[2], Yan Chen[2], Ruizhong Zhang[2]

[1]First Affiliated Hospital of Jinan University

[2]Department of Pediatric Surgery, Guangzhou Women & Children's Medical Center, Guangzhou Medical University

Correspondence to: Ruizhong Zhang at cowboy2006@163.com

URL: https://www.jove.com/video/58158
DOI: doi:10.3791/58158

Keywords: Immunology and Infection, Issue 140, Biliary atresia, silver nanoparticle, rhesus rotavirus, neonatal mouse, intraperitoneal injection, treatment

Date Published: 10/13/2018

Citation: Fu, M., Lin, Z., Lin, H., Tong, Y., Wang, H., Chen, H., Chen, Y., Zhang, R. A Silver Nanoparticle Method for Ameliorating Biliary Atresia Syndrome in Mice. *J. Vis. Exp.* (140), e58158, doi:10.3791/58158 (2018).

Abstract

Biliary atresia (BA) is a severe type of cholangitis with high mortality in children of which the etiology is still not fully understood. Viral infections may be one possible cause. The typical animal model used for studying BA is established by inoculating a neonatal mouse with a rhesus rotavirus. Silver nanoparticles have been shown to exert antibacterial and antiviral effects; their function in the BA mouse model is evaluated in this study. Currently, in BA animal experiments, the methods used to improve the symptoms of BA mice are generally symptomatic treatments given *via* food or other drugs. The aim of this study is to demonstrate a new method for ameliorating BA syndrome in mice by the intraperitoneal injection of silver nanoparticles and to provide detailed methods for preparing the silver nanoparticle gel formulation. This method is simple and widely applicable and can be used to research the mechanism of BA, as well as in clinical treatments. Based on the BA mouse model, when the mice exhibit jaundice, the prepared silver nanoparticle gel is injected intraperitoneally to the surface of the lower liver. The survival status is observed, and biochemical indicators and liver histopathology are examined. This method allows a more intuitive understanding of both the establishment of the BA model and novel BA treatments.

Video Link

The video component of this article can be found at https://www.jove.com/video/58158/

Introduction

BA is a form of cholestasis characterized by persistent jaundice and has high mortality in the absence of liver transplantation. Viral infections are closely associated with the pathogenesis of BA. The cytomegalovirus, reovirus, and rotavirus have all been suggested as pathogens in BA[1,2,3]. During the neonatal period, the response of the immature immune system to a viral infection results in immune dysregulation against extra- and intrahepatic bile ducts, leading to biliary epithelial cell apoptosis, inflammatory cell infiltration in the portal area, intrahepatic and extrahepatic bile duct obstruction, and finally, liver fibrosis[4,5,6].

The commonly used animal model for BA studies involves the inoculation of a neonatal mouse with the rhesus rotavirus (RRV). The mouse typically develops jaundice after 5 - 6 days, showing a low body weight and acholic stools. The role of the immune response in the disease process is critical, especially for natural killer (NK) cells; the depletion of these cells with anti-NKG2D antibody greatly reduces BA-induced damage[7]. Furthermore, other cells, including $CD4^+$ T cells, $CD8^+$ T cells, dendritic cells, and regulatory T cells, have all been shown to play roles in the disease[8,9,10,11]. All data suggest the indispensable nature of the immune system in the course of BA.

Silver nanoparticles (AgNPs) have been demonstrated to have beneficial effects against some infectious diseases, including bacterial infections[12] and viral infections[13,14,15]. However, other than dermatological usage, few studies have used AgNPs in a clinical treatment, mostly because of their potential toxicity. In animal experiments, researchers have generally studied the efficacy of AgNPs administered *via* oral[16] or intravenous methods[17]. However, no other researchers have studied the efficacy of AgNPs administered *via* an intraperitoneal (i.p.) injection in neonatal mouse experiments, which is a simple and rapid method leading to a more direct effect on the liver and bile ducts while reducing the toxicity to other systems, such as the immune system. AgNPs have been shown to affect NK cell activity[18]; therefore, we tested the therapeutic effects of AgNPs administered *via* i.p. injection in the BA mouse model.

Protocol

All animal experimental protocols have been approved by the Institutional Animal Care and Use Committee of the Sun Yat-Sen University Laboratory Animal Center (#IACUC-DB-16-0602).

1. Establishing the Biliary Atresia Mouse Model

1. Maintain pregnant BALB/c mice in a specific pathogen-free environment under a 12 h dark/light cycle at 25 °C, with access to autoclaved chow *ad libitum*.
2. To prepare the RRV strain MMU 18006, amplify the virus in MA104 cells and measure the viral titers by a plaque assay[19].
   NOTE: MA104 cells are cultured in Dulbecco's modified Eagle's medium (DMEM) with 10% fetal bovine serum (FBS) in an incubator with a humidified atmosphere containing 5% CO_2. The amplification steps are briefly outlined below.
   1. Infect MA104 cells (1.5×10^7) in a 150 cm^2 culture flask with trypsin-activated RRV [1.5×10^6 plaque-forming units (PFU)] in 30 mL of serum-free medium. Incubate the infected cells for 3 days in a humidified incubator at 37 °C with 5% CO_2.
   2. Lyse the infected cells in the culture flask by three freeze-and-thaw cycles, with 20 min in a -80 °C freezer for each freeze phase and, then, thawing the cells back to room temperature; the cell-associated virus particle will release into the supernatant. Then, collect and transfer the cell lysate and culture supernatant into a 15 mL conical tube.
   3. Remove large cellular debris from the lysate by low-speed centrifugation (300 x *g* at 4 °C for 3 min). Then, transfer the supernatant containing the virus (approximately 6 mL) into a new 15 mL conical tube for animal experiments.
      NOTE: The RRV is then ready to be titered, aliquoted, and stored or used for additional rounds of amplification. Long-term exposure to room temperature will reduce the viral infection capacity; the virus should be placed on ice and stored at -80 °C or in liquid nitrogen.
3. Load the RRV into a small-volume (1 mL) insulin syringe with a 29 G needle for the neonatal mouse injection.
   NOTE: The thick needles of volumetric syringes easily lead to drug leakage.
4. Within 24 h of birth, administer to each neonate 20 µL of 1.2×10^5 PFU/mL RRV *via* the i.p. route; use the same volume of saline as the control.
   NOTE: The syringe used in this experiment is a 1 mL insulin syringe. Infected mice that were not fed by their mothers died within the first 2 days due to other reasons were not included in the analysis.
5. Observe all neonatal mice closely and weigh them daily. Typically, on the sixth day after the RRV inoculation, jaundice appears on the ears and bare skin, the stool becomes clay-colored, and the fur becomes oily, suggesting the establishment of the BA model; check for these symptoms.
   NOTE: BA can be confirmed by a liver tissue section examination with H & E and immunohistochemical stating. The BA mice are then ready for the AgNP treatment.
   CAUTION: The protocol presented is for use with contemporary animal and human RV strains, which must be handled under Biosafety Level 2 (BSL-2) conditions.

2. Silver Nanoparticle Synthesis

1. Prepare and characterize the AgNPs as previously described[12,20].
   NOTE: The details of preparing and characterizing the AgNPs have been described in publications by C. M. Che's team at the Department of Chemistry, the University of Hong Kong[12,20]. The final concentration of the solution was 1 mM. The mean diameter of the AgNPs was 10 nm (ranging 5 to 15 nm) and confirmed by electron microscopy.

3. Preparation of the Silver Nanoparticle Collagen Mixture

NOTE: The AgNP collagen mixture is prepared and characterized as previously described[21] and stored at 4 °C. All procedures must be performed on ice.

1. First, for the collagen preparation, add 490 µL of type I collagen (4 mg/mL) to a 1.5 mL tube and place it on ice.
2. Add 100 µL of phosphate-buffered saline (PBS, 10x) to the collagen and mix it with a pipette.
   1. To prepare 1 L of 10x PBS buffer, combine 80 g of NaCl, 2 g of KCl, and 35.8 g of $Na_2HPO_4 \cdot 12H_2O$ to 2.4 g of KH_2PO_4 and store the buffer at room temperature.
3. Then, add 10 µL of NaOH (0.2 M) to the above solution.
   1. To prepare 0.2 M NaOH, add 8 g of NaOH powder to 1 L of distilled water.
4. Finally, add 400 µL of AgNPs (1 mM) to the collagen and mix them with a pipette.
   NOTE: Add the AgNPs last for an even mixing. The AgNP collagen mixture should be stored at 4 °C; otherwise, it easily solidifies at room temperature.

4. Mouse Injection Method

1. Administer the infected neonatal mice in the treated RRV group with an i.p. injection of 50 µL of the AgNP collagen mixture after the appearance of jaundice; perform a second injection 3 d later.
   NOTE: The mice in the control RRV (infected control) group are given the same volume of saline, and the mice in the normal control group are not given any treatment.
2. At the beginning of the injection, press the mouse's leg with the ring finger obliquely over the right thigh, and introduce the needle slowly at a 15° angle (**Figure 1**). Upon reaching the surface of the lower edge of the liver (**Figure 2**), about 0.5 cm in, inject the AgNP collagen mixture; then, withdraw the needle slowly.
   NOTE: Be careful not to introduce any air into the syringe as, then, the neonatal mouse may be killed. In neonatal mice, the stomach and spleen are in the left abdomen, and the stomach is full of milk. If the injection is administered from this side, the needle could easily enter either the stomach, causing milk to flow into the abdominal cavity, or the spleen, causing bleeding.

CAUTION: Pay attention to the needle to prevent any finger injuries, and be sure to replace the needle cap, remove the needle, and place it in a sharps container.
3. After all the injections, keep the mice out of their cages for 10 min to allow the AgNP collagen mixture to gel and to prevent the mother from licking the injection site. Then, return the mice to their cages.
4. Observe and record the physical appearances of all mice daily, including jaundice and body weight, as well as the survival rate.

5. Blood Sample Collection

NOTE: Blood samples of approximately 120 µL are collected by inserting the needle into the heart. After centrifugation, the serum is collected (approximately 70 µL) for liver function testing. The blood collection method is as follows.

1. Anesthetize the mice on the ninth and 12th day after the RRV inoculation (which is 3 days after the AgNP treatment) using 0.5-2.5% sevoflurane.
2. Immobilize the limbs of the mouse and sterilize the upper and lower abdomen with 75% alcohol.
3. Expose the diaphragm by cutting the mouse skin, muscle, and peritoneum along the midline to the xiphoid with scissors; use a sterile cotton swab to remove the gastrointestinal tract to fully expose the diaphragm muscle.
4. Insert the needle (with a 1 mL unloaded insulin syringe) into the left ventricle of the heart and slowly pull back the syringe plunger to obtain the maximum blood volume. Then, transfer the blood to a 1.5 mL tube.
5. Allow the tube to stand for 30 min at room temperature and centrifuge it for 5 min at 400 x *g*. Then, using a transfer pipette, collect and save the serum for further use.
   NOTE: Avoid damaging the diaphragm, as diaphragm defects easily lead to pneumothorax, death, and blood coagulation, thereby preventing the blood sample collection.

6. Biochemical Parameter Detection

1. Use the serum collected in step 5.5 for a biochemical parameter detection.
2. Use an automated biochemical analyzer to detect the following biochemical parameters: alanine aminotransferase (ALT), aspartate aminotransferase (AST), alkaline phosphatase (ALP), total protein (TP), albumin (ALB), globulin (GLO), total bilirubin (TBIL), direct bilirubin (DBIL), indirect bilirubin (IBIL), and total bile acids (TBA).

7. Extrahepatic Cholangiography to Observe the Extrahepatic Bile Duct Patency

NOTE: Perform the entire process under a dissection microscope.

1. Fully expose the liver, gallbladder, and extrahepatic bile ducts with a cotton swab.
2. Observe and photograph the appearance of the liver and bile ducts under a dissection microscope.
3. Use ophthalmic forceps to gently hold the bottom of the gallbladder.
4. Load a 1 mL syringe with methylene blue solution (0.05 wt.% in H_2O). Slowly insert the syringe needle into the gallbladder cavity; then, grasp the needle with the ophthalmic forceps, and slowly infuse 10–20 µL of methylene blue.
5. Observe under a microscope whether the blue color passes through the extrahepatic bile ducts to the jejunum and take a photograph.

8. Collection of Fresh Liver Samples for Hematoxylin and Eosin Staining

1. Fix the fresh mouse liver tissues overnight in 10% formalin.
2. Then, embed the fixed liver tissues in paraffin and section them.
3. Dewax the sections, rehydrate them with an ethanol series (such as 100%, 95%, 80%, and 70% ethanol in distilled water, each for 5 min), stain the tissue sections with hematoxylin, subject them to a 1% hydrochloric acid alcohol differentiation, and finally, stain the sections with eosin.
4. Finally, observe the histopathology of the liver under a 40X microscope.

9. Immunohistochemical Staining of the Hematoxylin and Eosin-stained Tissue Sections

1. After dewaxing and rehydrating the sections, perform an antigen retrieval by submerging the sections in Tris-EDTA buffer (10 mM Tris base, 1 mM EDTA solution; pH 9.0) and heating them in a microwave for 10 min at 95 °C.
2. Remove endogenous peroxidase by exposing the tissue sections for 10 min to a 3% hydrogen peroxide solution.
3. Treat the sections with 5% goat serum, to block nonspecific binding.
4. Add primary antibodies rabbit-mouse NKG2D (1:100) to the sections, and incubate them overnight at 4 °C.
5. Incubate the sections with the appropriate secondary antibodies (HRP-labeled polymer anti-rabbit system) for 30 min at room temperature.
6. Visualize the immunohistochemical staining using 3,3'-diaminobenzidine (DAB) as chromogen.
7. Observe the sections under a 40X microscope, acquire images, and proceed to analyze them as desired.

10. Flow Cytometric Analysis

1. Gently mince the liver tissue, pass it through a 70 µm cell strainer, and centrifuge it 2x at 270 x *g* at 4 °C for 4 min.
2. Resuspend the cell pellet in RPMI 1640 medium and analyze it by two-color immunofluorescence using monoclonal antibodies.

3. Perform cellular phenotyping using specific cell-surface markers, including fluorescein isothiocyanate- and phycoerythrin-conjugated anti-NKp46 (NK lymphocytes; 1:1,000) and anti-CD4 (T-cell subtype; 1:1,000), with a flow cytometer and analyze the data with flow cytometry data analysis software.
4. Select cell populations according to forward/side scatter, gate according to the isotype controls to account for any background fluorescence, and subject the data to a secondary analysis based on the fluorescence signals from individual antibodies.

Representative Results

Based on the established BA mouse model, the infected neonatal mice were administered an i.p. injection of the prepared AgNP collagen mixture 2x after exhibiting jaundice. Mouse survival was checked for daily, and liver function testing, liver pathology, and flow cytometry were performed. Compared to the untreated control BA mice, the AgNP-treated mice showed reduced jaundice and maintained their normal body weight (**Figure 3**). The levels of bilirubin metabolism and hepatic transaminase dropped to normal control values, suggesting that the AgNPs greatly improved the liver function (**Table 1**). Extrahepatic cholangiography (**Figure 4**) with methylene blue staining confirmed the bile duct patency after the AgNP treatment. H&E staining (**Figure 5**) showed a significantly decreased inflammatory cell infiltration in the hepatic portal area of mice treated with AgNPs, compared to the control mice. The flow cytometry results showed significantly less NK cells in the livers after the AgNP treatments (both on days 9 and 12) than in the RRV mice (**Figure 6**). Immunohistochemical staining revealed a substantially reduced expression of the NK cell marker NKG2D (**Figure 7**) in the portal triad of the AgNP-treated mice, compared to the RRV mice.

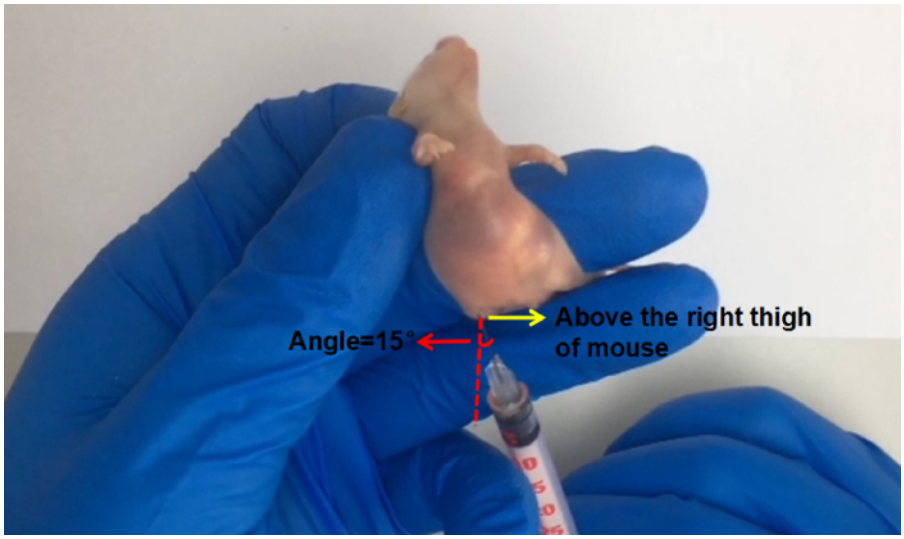

Figure 1: Initial syringe penetration position. The red dotted line indicates the line parallel to the abdomen of the P6 neonatal mouse; the yellow arrow indicates the needle point; the red arrow indicates the needle angle. Please click here to view a larger version of this figure.

Figure 2: Needle reaching the surface of the lower edge of the liver. The yellow dotted line indicates the lower edge of a mouse liver; the red arrow indicates the needle position during the injection. Please click here to view a larger version of this figure.

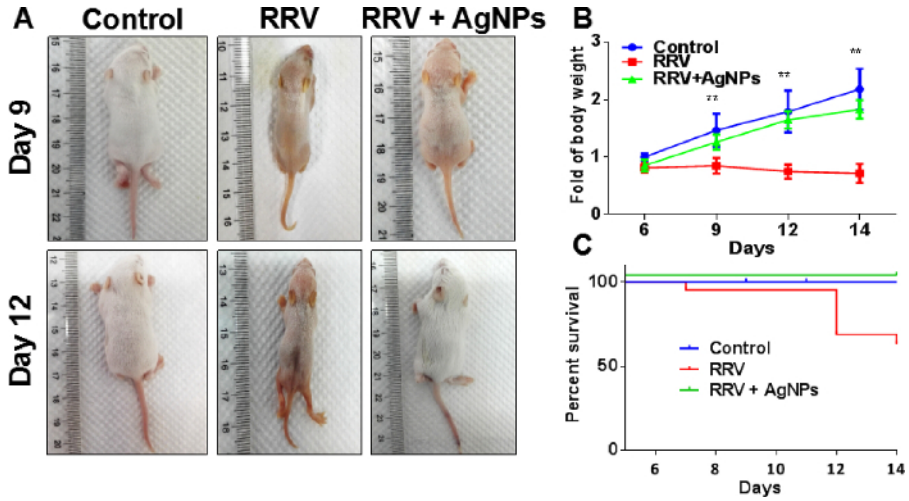

Figure 3: Effect of AgNPs on BA syndrome in an experimental BA mouse model. (**A**) This panel shows the appearance of neonatal mice on days 9 and 12 after an injection with RRV alone and 3 days and 6 days after an injection with AgNPs (RRV + AgNPs). (**B**) This panel shows the weight of the mice in each group at different time points; the *x*-axis indicates the number of days after the mouse was born and the *y*-axis indicates the fold-change in body weight. ***P* < 0.01 with Student's *t*-test comparing the RRV + AgNp group to the RRV control group; *n* = 16 in the control group, *n* = 18 in the RRV group, and *n* = 17 in the RRV + AgNP group. (**C**) This panel shows the survival rate of the mice in each group. This figure has been modified from Zhang *et al.*[18]. Please click here to view a larger version of this figure.

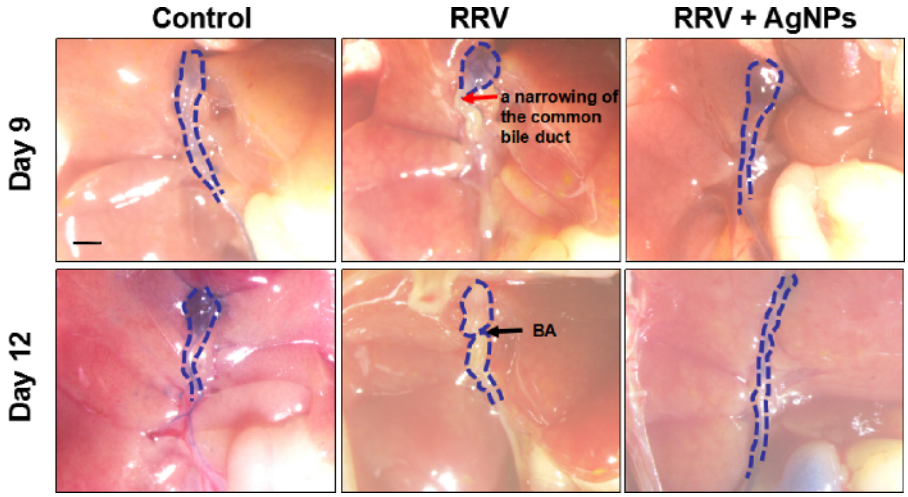

Figure 4: Extrahepatic cholangiography. A contrast agent was used to detect the patency of the extrahepatic bile ducts and to capture images. The blue dotted line indicates the direction of the extrahepatic bile duct; the red arrow indicates a narrowing of the common bile duct; the black arrow indicates BA. Scale bar = 1 mm. Please click here to view a larger version of this figure.

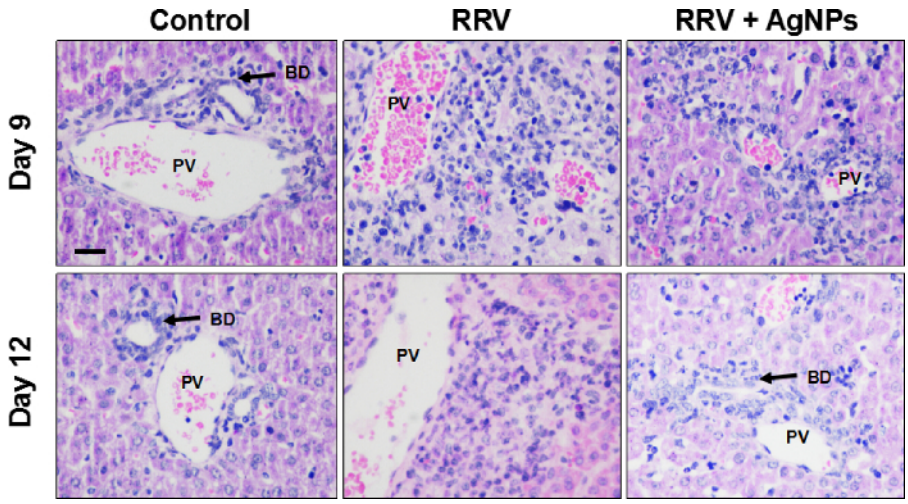

Figure 5: H&E staining. Liver tissues of the mice in each group on days 9 and 12 were collected, fixed, sectioned, and stained with H&E. Abbreviations: PV = portal vein, BD = bile duct. Scale bar = 50 μm. This figure has been modified from Zhang *et al.*[18]. Please click here to view a larger version of this figure.

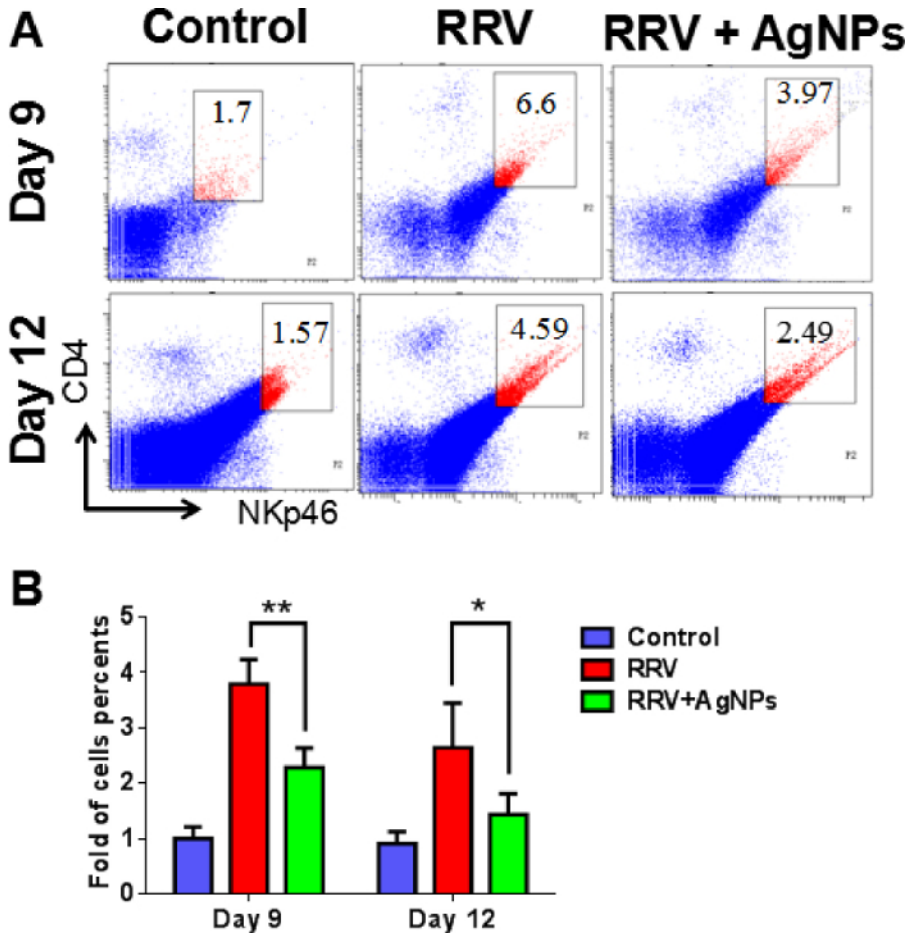

Figure 6: Percentage of NK cells in the liver tissue. (**A**) The livers of mice were processed into cell suspensions on days 9 and 12, and the proportion of NK cells was detected by flow cytometry. (**B**) This panel shows the percentage of NK cells ($NKp46^{+}CD4^{+}$) in each group at different time points after the AgNP injection. The *y*-axis indicates the fold-change in the percentage of NK cells, which was calculated relative to the percentages of the control group on day 9 and day 12.$^{**}P < 0.01$ and $^{*}P < 0.05$, with Student's *t*-test comparing the RRV + AgNp group to the RRV control group, $n = 10$ in each group. This figure has been modified from Zhang *et al.*[18]. Please click here to view a larger version of this figure.

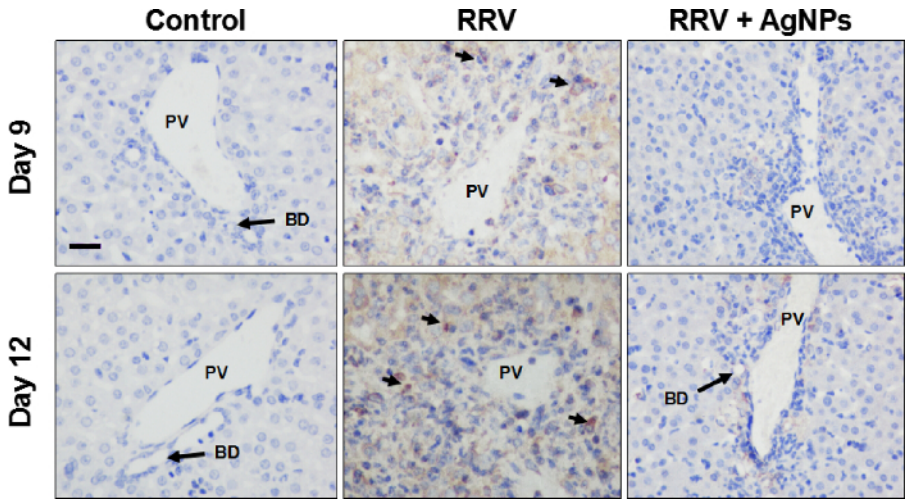

Figure 7: Immunohistochemical staining for the NK cell marker NKG2D in the portal area of the mice in each treatment group. The expression of the NK cell marker NKG2D in the portal area of the mice in each treatment group was detected by immunohistochemical staining. The long arrows indicate bile ducts; the short arrows indicate NK cells. Abbreviations: PV: portal vein, BD: bile duct. Sscale bar = 50 μm. This figure has been modified from Zhang *et al.*[18]. Please click here to view a larger version of this figure.

	ALT(U/L)	AST(U/L)	ALP(U/L)	TP(g/L)	ALB(g/L)	GLO(g/L)	A/G	TBIL(μM)	DBIL(μM)	IBIL(μM)	TBA(μM)
Control (n=10)	36.7±7.5	175.0±63.4	441.7±167.6	43.7±0.9	25.5±1.4	18.2±1.0	1.4±0.13	3.5±0.71	0.58±0.73	2.9±1.0	12.5±3.6
RRV (n=10)	87.2±53.5	784.4±423.9	1161.7±423.9	43.4±11.0	22.9±5.0	18.0±3.4	1.2±0.3	1545±58.2	147.3±51.7	7.2±7.2	464.1±120.6
RRV+AgNps (n=10)	37.8±14.2*	175.0±116.8**	401.9±115.1**	41.6±2.1**	24.4±1.4	17.2±1.2	1.4±0.1	1.2±0.6**	1.0±0.4**	0.4±0.4**	5.7±3.6**

Table 1: Clinical laboratory examination of liver function-related molecule serum levels. Peripheral blood was used to measure the liver function in the mice in each group. ALT: alanine aminotransferase, AST: aspartate aminotransferase, ALP: alkaline phosphatase, TP: total protein, ALB: albumin, GLO: globulin, TBIL: total bilirubin, DBIL: direct bilirubin, IBIL: indirect bilirubin, and TBA = total bile acids. *P < 0.05 and **P < 0.01, with Student's t-test for each cohort compared to the RRV alone group, n = 10 in each group. All biochemical indicator data are displayed as the mean ± SD. All mice in the three groups were 12 days old. This table has been modified from Zhang *et al.*[18]. Please click here to download this file.

Discussion

AgNPs exhibit potent broad-spectrum antibacterial properties and a strong permeability[22]; additionally, they are used to produce a range of antibacterial medical products[23]. However, AgNPs can take a long time to clear once they accumulate in organs, and this persistence may lead to toxic effects[24,25]. A previous study examined the acute toxicity and genotoxicity of AgNPs after a single i.v. injection in a rat experiment, and the results showed that AgNPs could cause acute liver and kidney damage. AgNPs accumulated in the main immune system organs, including the thymus and the spleen[17]. In this mouse BA model, the treatment with AgNPs ameliorated BA syndrome, which our data suggest is partially mediated by NK cell inhibition. However, the long-term effects of AgNPs require a further investigation, to assess the potential toxicity to the mouse development and immune regulation.

In terms of the method, some additional notes for a successful surgery are as follows: (i) The process of preparing the AgNP collagen mixture must be carried out on ice because, at room temperature, the AgNP collagen mixture will quickly become a semi-solid gel, which cannot be used for injections. After the preparation, the AgNP collagen mixture should be stored at 4 °C. (ii) Only 1 mL insulin syringes should be used because of the small diameter, which reduces the leakage of the injected drug. (iii) Previous studies have generally examined the effect of AgNPs administered orally[16] or *via* intravenous injection[17]. In our animal experiments, the experimental subjects are neonatal mice; thus, intravenous injection is almost impossible, and we used an i.p. injection. The injection of AgNPs improved the symptoms of BA in the mice. (iv) At the beginning of the injection, the lower limbs of the mouse are fixed by hand to prevent the mouse from moving. This method ensures that the right amount of the drug is injected into the abdominal cavity without any leakage and further guarantees the efficacy of the experiment. (v) In neonatal mice, the stomach and spleen are in the left abdomen, and the stomach is full of milk. To inject the AgNP mixture to the surface of the lower edge of the liver, the needle is inserted from above the right thigh of the mouse. If the needle is inserted from the left side, it could easily puncture either the stomach, causing milk to flow into the abdominal cavity, or the spleen, causing bleeding. (vi) Because the abdominal wall in neonatal mice is thin, drug leakage can be prevented by diagonally advancing the needle at a 15° angle close to the abdominal wall to reach the lower edge of the liver.

We have observed the encouraging effect of the AgNPs in this RRV-induced mouse BA model. Together with previous studies that used AgNPs in the treatments of varying virus infections and diseases, these AgNP data suggest the possibility of an *in vivo* application in anti-virus infections. The limitation of these experiments is that the pharmacokinetics of AgNPs is not totally clear as due to a lack of measurement methods for the AgNPs, which makes the control of AgNP dosages difficult. Further study is also needed for the intracellular target of the AgNPs, which will help us to understand the mechanism and reduce the side-effects in future disease treatments.

Disclosures

The authors have nothing to disclose.

Acknowledgements

The AgNPs used here were a gift from C. M. Che in the Department of Chemistry, the University of Hong Kong. This work was funded by the National Natural Science Foundation of China (No. 81600399) and the Science and Technology Project of Guangzhou (No.201707010014).

References

1. Szavay, P. O., Leonhardt, J., Czechschmidt, G., Petersen, C. The role of reovirus type 3 infection in an established murine model for biliary atresia. *European Journal of Pediatric Surgery.* **12** (04), 248-250 (2002).
2. Coots, A. *et al.* Rotavirus infection of human cholangiocytes parallels the murine model of biliary atresia. *Journal of Surgical Research.* **177** (2), 275-281 (2012).
3. Shanmugam, N. P., Jayanthi, V. Biliary atresia with cytomegalovirus. *Indian Pediatrics.* **49** (2), 157 (2012).
4. Mack, C. L., Feldman, A. G., Sokol, R. J. Clues to the Etiology of Bile Duct Injuryin Biliary Atresia. *Seminars in Liver Disease.* **32**, 307-316 (2012).
5. Muraji, T., Suskind, D. L., Irie, N. Biliary atresia: a new immunological insight into etiopathogenesis. *Expert Review of Gastroenterology & Hepatology.* **3** (6), 599-606 (2009).
6. Sokol, R. J., Mack, C. Etiopathogenesis of Biliary Artesia.*Seminars in Liver Disease.* **21**, 517-524 (2001).
7. Shivakumar, P., Sabla, G. E., Whitington, P., Chougnet, C. A., Bezerra, J. A. Neonatal NK cells target the mouse duct epithelium *via* Nkg2d and drive tissue-specific injury in experimental biliary atresia. *Journal of Clinical Investigation.* **119** (8), 2281-2290 (2009).
8. Mack, C. L. *et al.* Oligoclonal expansions of CD4+ and CD8+ T-cells in the target organ of patients with biliary atresia. *Gastroenterology.* **133** (1), 278-287 (2007).
9. Shivakumar, P. *et al.* Effector Role of Neonatal Hepatic CD8 + Lymphocytes in Epithelial Injury and Autoimmunity in Experimental Biliary Atresia. *Gastroenterology.* **133** (1), 268-277 (2007).
10. Saxena, V. *et al.* Dendritic Cells Regulate Natural Killer Cell Activation and Epithelial Injury in Experimental Biliary Atresia. *Science Translational Medicine.* **3** (102), 102ra194 (2011).
11. Miethke, A. G. *et al.* Post-natal paucity of regulatory T cells and control of NK cell activation in experimental biliary atresia. *Journal of Hepatology.* **52** (5), 718-726 (2010).
12. Tian, J. *et al.* Topical delivery of silver nanoparticles promotes wound healing. *ChemMedChem.* **2** (1), 129-136 (2010).
13. Lu, L. *et al.* Silver nanoparticles inhibit hepatitis B virus replication. *Antiviral Therapy.* **13** (2), 253-262 (2008).
14. Xiang, D. *et al.* Inhibition of A/Human/Hubei/3/2005 (H3N2) influenza virus infection by silver nanoparticles *in vitro* and *in vivo*. *International Journal of Nanomedicine.* **8** (Issue 1), 4103-4114 (2013).
15. Elechiguerra, J. L. *et al.* Interaction of silver nanoparticles with HIV-1. *Journal of Nanobiotechnology.* **3** (1), 1-10 (2005).
16. Nallanthighal, S. *et al.* Differential effects of silver nanoparticles on DNA damage and DNA repair gene expression in Ogg1-deficient and wild type mice. *Nanotoxicology.* **11** (8), 1-16 (2017).
17. Wen, H. *et al.* Acute toxicity and genotoxicity of silver nanoparticle in rats. *PLoS One.* **12** (9), e0185554 (2017).
18. Zhang, R. *et al.* Silver nanoparticle treatment ameliorates biliary atresia syndrome in rhesus rotavirus inoculated mice. *Nanomedicine.* **13** (3), 1041-1050 (2017).
19. Arnold, M., Patton, J. T., McDonald, S. M. Culturing, Storage, and Quantification of Rotaviruses. *Current Protocols in Microbiology.* **Chapter 15** Unit 15C.13 (2009).
20. Liu, X. *et al.* Silver nanoparticles mediate differential responses in keratinocytes and fibroblasts during skin wound healing. *ChemMedChem.* **5** (3), 468-475 (2010).
21. Zhang, R. *et al.* Silver nanoparticles promote osteogenesis of mesenchymal stem cells and improve bone fracture healing in osteogenesis mechanism mouse model. *Nanomedicine.* **11** (8), 1949-1959 (2015).
22. Wu, J., Hou, S., Ren, D., Mather, P. T. Antimicrobial properties of nanostructured hydrogel webs containing silver. *Biomacromolecules.* **10** (9), 2686-2693 (2009).
23. Xu, L. Genotoxicity and molecular response of silver nanoparticle (NP)-based hydrogel. *Journal of Nanobiotechnology.* **10** (1), 16-16 (2012).
24. Dobrzyńska, M. M. *et al.* Genotoxicity of silver and titanium dioxide nanoparticles in bone marrow cells of rats *in vivo*. *Toxicology.* **315** (1), 86-91 (2014).
25. Mohamed, H. R. H. Estimation of TiO 2 nanoparticle-induced genotoxicity persistence and possible chronic gastritis-induction in mice. *Food & Chemical Toxicology.* **83** (9), 76-83 (2015).

